Dual-Channel Approach to Photonic Modulators in Silicon-on-Insulator Technology

V. M. N. Passaro, F. De Leonardis °, and F. Dell'Olio

Photonics Research Group, Dipartimento di Elettrotecnica ed Elettronica, Politecnico di Bari, via Edoardo Orabona n. 4, 70125 Bari, Italy

° Dipartimento di Ingegneria dell'Ambiente e per lo Sviluppo Sostenibile, Politecnico di Bari, viale del Turismo n. 8, 74100 Taranto, Italy

The well-known main methods to modulate the refractive index in silicon-based waveguides are the thermo-optic effect and the plasma dispersion effect. The latter is much faster, allowing modulation frequencies of the order of gigahertz and it is used to change both the real refractive index and optical absorption coefficient. In this paper, we analyze an improved architecture of a depletion-type device for varying the refractive index of Silicon-on-Insulator waveguides by using a four terminal p-n junction diode. The modeling and design of an optimized architecture of depletion-type photonic modulator in silicon-on-insulator is presented and discussed. Highly compact structure is demonstrated by using a novel interferometer dual-channel approach.

Device structure

Nowadays, there is an increasing interest in Silicon Photonics [1], in particular for silicon modulators [2]. For instance, Fig. 1(a) illustrates the device structure presented in literature by Gardes et al. [3]. It is a depletion-type vertical optical phase modulator integrated in a low loss Silicon-on-Insulator (SOI) rib waveguide. The device has an asymmetrical p-n structure where two slab n^+ silicon regions work as a common cathode and two p^+ polysilicon regions are joined as a common anode (four terminals). Both n^+ and p^+ regions are modeled as highly doped regions with peak doping concentrations of $1x10^{19}$ ion/cm^3. The optimized structure is based on a silicon thickness of 0.45 μm, etched rib waveguide 0.415 μm wide and a slab thickness of 0.1μm. The silicon slab and the bottom part of the rib have an n-type background doping concentration of $4x10^{17}$ ion/cm^3 and the top part of the rib has a p-type uniform doping concentration of $2x10^{17}$ ion/cm^3 (uniform profile, see Fig. 1a). The oxide thickness is chosen to be 1μm which ensures good optical confinement and a top silicon oxide cladding layer covers the whole structure.

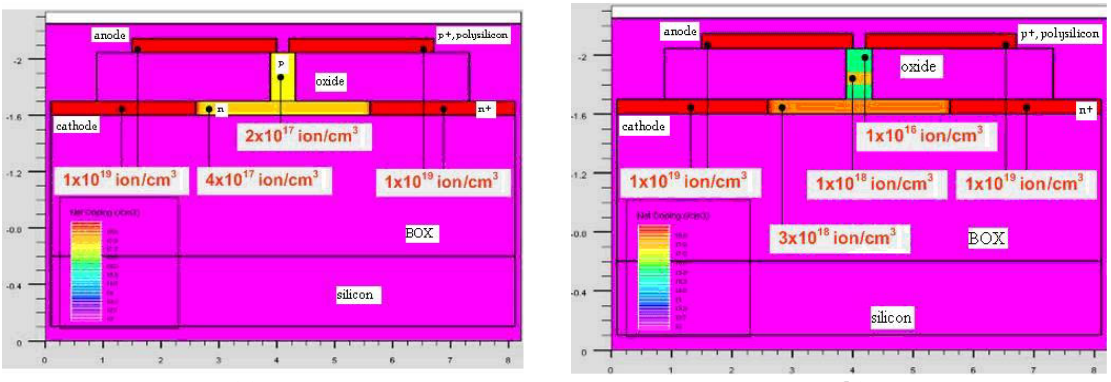

(a) (b)

Fig. 1. (a) Cross section of structure by Gardes et al. [3] and (b) modified structure of this paper.

The n^+ doped regions are situated on both sides of the wave guiding region, in the slab, 1.5 μm away from the centre of the waveguide. In general, the design was optimized in order to achieve birefringence free propagation (equal effective index for quasi-TM and quasi-TE waves in the rib), single mode condition, optimum value and positioning of *n*-type and *p*-type doping, maximum bandwidth and minimum losses. In particular, the rib width has a direct influence on the capacitance of the device, as the p-n junction is situated in the rib of the waveguide, so diminishing the rib width reduces the relevant capacitance.

Moreover, Fig. 1(b) shows the modified structure investigated in this paper. Although the four terminal approach and all sizes are the same as before, the doping profile inside the rib has been modified by including a peak *p*-type doping at center ($1x10^{18}$ ion/cm^3 over 75 nm) and reducing the *p*-type doping in the rest of the rib ($1x10^{16}$ ion/cm^3 over 110 nm at the rib top and over 165 nm at rib bottom), and increasing the *n*-type doping inside the silicon slab ($3x10^{18}$ ion/cm^3). By this doping profile, a reduction of carrier absorption inside the rib, an increase of index modulation due to stronger changes of free carrier concentrations, and an increase of breakdown voltage larger than 10 V can be simultaneously achieved together with the other advantages already mentioned (single mode, birefringence free). These results are obtained without inducing any optical loss increase, given by 2 dB/cm for 0V and 1 dB/cm for 10V of bias voltage.

The importance of this modified structure is clear when we consider the device as inserted in both arms of a 1x1 Mach Zehnder (MZ) interferometer. In Fig. 2(a) the push-pull MZ interferometer is sketched by using the depletion device of Fig. 1(a). Here four phase shifters of the same geometry are required, two of them represent the AC depletion devices, the next two are DC phase shifters and bias the device by introducing a static π-phase shift in one arm. The length of a depletion phase shifter was calculated to be 2.5 mm in order to achieve a π-phase shift when a reverse bias of 10V is applied [3]. Then, a total length of about 5 mm was obtained. In Fig. 2(b) the MZ interferometer is sketched as modified by including the device structure of Fig. 1(b) in the right arm and the same structure of Fig. 1(a) in the left arm (named as *dual-channel approach*). Each phase modulator is 2.52 mm long. The ”OFF state” is achieved by driving the AC modulator on the left at a reverse bias of 3 V and the AC modulator on the right at 4 V: this enables destructive interference at the output. The ”ON state” corresponds to AC modulators having a bias of 10V (on the left) and 0V (on the right) respectively, allowing constructive interference. Since the interferometer can be achieved by using only two AC modulators, the MZ total length should be significantly reduced.

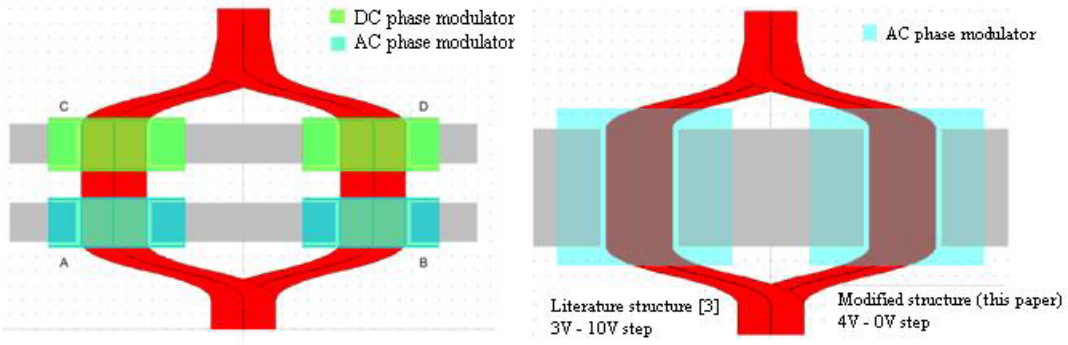

(a) (b)

Fig. 2. (a) Structure by Gardes et al. [3] and (b) dual-channel interferometer architecture.

Device modeling

The device has been electrically modeled for both its static and dynamic behavior using a commercial simulation package [4], by solving the equations which describe the semiconductor physics such as Poisson's equation and charge continuity equations for holes and electrons. This approach has been used to find the free carrier concentrations in the wave-guiding region of the device for both DC and transient biasing conditions. From those concentrations, both refractive index and absorption coefficient changes have been evaluated by using the well known Soref's equations [5]. Fig. 3 shows the refractive index change versus position along the rib for both structures (uniform and modified doping profile), respectively. An index change larger up to six times than that provided in [3] is so demonstrated.

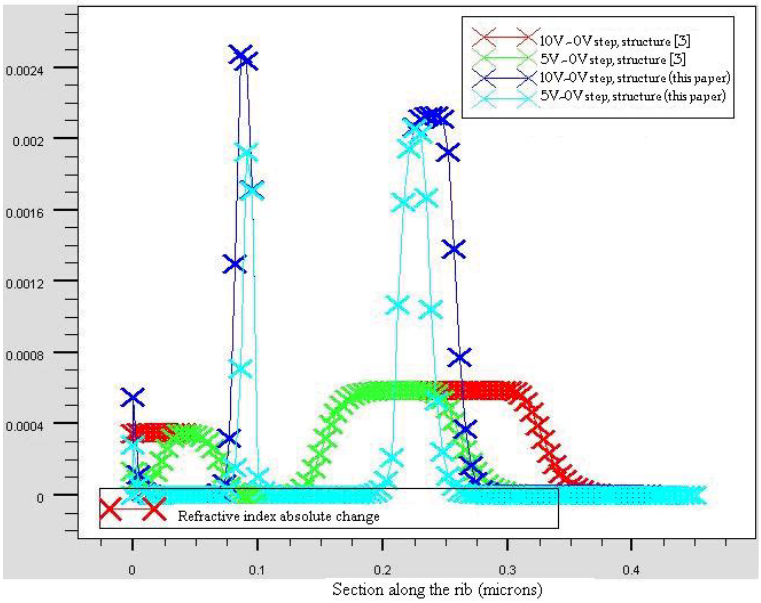

Fig. 3. Refractive index change versus rib position for both structures.

However, a very moderate increase of absorption is revealed by simulations, so keeping still low the losses.

The device has been optically modeled using the full-vectorial beam propagation method [6] at the wavelength of 1.55μm. By considering the refractive index change provided by the electrical simulation of the free carrier distribution in the p-n device, as in Fig. 3, it is possible to predict the effective index change of the waveguide for different applied voltages. The same approach has been used to characterize the phase shift against transient time, i.e. the device dynamic operation.

Fig. 4(a) shows the phase shift as a function of applied voltage achieved for the two polarizations, quasi-TE or quasi-TM, using the modified structure. Then, a phase shift of 172° for quasi-TE or 225° for quasi-TM can be obtained by applying 10 V over a simple phase shifter 2.5 mm long.

Moreover, in Fig. 4(b) the phase switch is sketched versus transient time for dual-channel MZ device, 2.52 mm long, biased in OFF-ON-OFF state for both polarizations. This dynamic study clearly gives a switching time of 8 ps and, then, a device bandwidth of about 60 GHz.

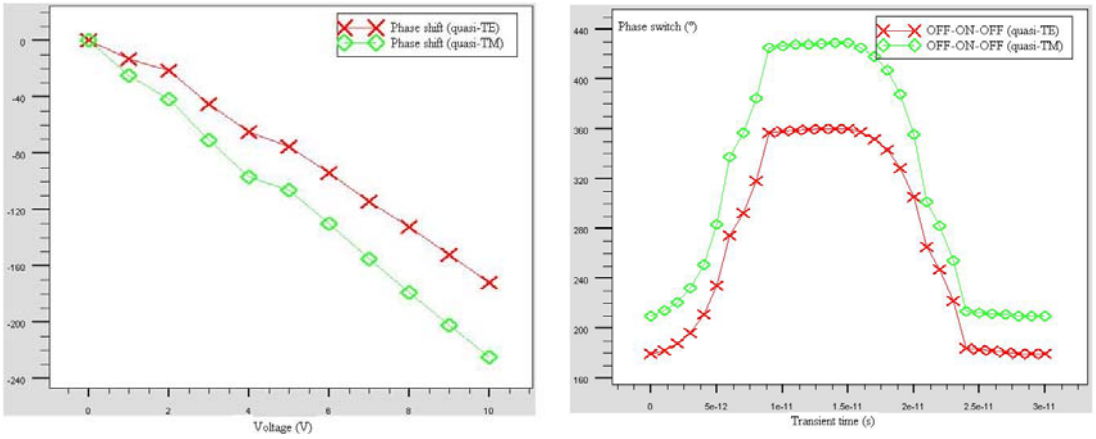

(a) (b)

Fig. 4. (a) Phase shift versus applied voltage and (b) dual-channel MZ phase switch versus transient time.

Conclusion

In this paper we have investigated an optimized architecture of a 2.52 mm long optical modulator based on a p-n junction integrated in a SOI rib waveguide for 1.55μm operation wavelength. The refractive index and the absorption coefficient of the rib waveguide are changed using the free carrier dispersion effect via depletion of a p-n junction. The doping profile inside the rib has been modified in order to achieve very large refractive index change (up to six times than in the uniform profile used in literature) and, then, large phase shifts while keeping low the absorption coefficient changes and the relevant losses. By using this optimized structure in one arm of a Mach-Zehnder interferometer and the uniform doping structure in the other arm (dual-channel approach), high performance and highly compact device has been theoretically demonstrated, including a length of about 2.52 mm, low switching time (8 ps instead of 7 ps) and large bandwidth, about 60 GHz.

References

[1] G. T. Reed, “The optical age of silicon”, Nature, vol. 427, pp. 595-596, 2004.

[2] G. T. Reed, C. E. Png, “Silicon Optical Modulators”, Materials Today, vol. 8, pp. 40-50, 2005.

[3] F.Y. Gardes, G.T. Reed, N.G. Emerson, C.E. Png, “A sub-micron depletion-type photonic modulator in silicon on insulator”, Opt. Express, vol. 13, pp. 8845-8854, 2005.

[4] ATLAS by Silvaco International Corporation, ver. 4.3.0.r, single license, 2004.

[5] R. A. Soref, B. R. Bennett, “Kramers-Kronig analysis of E-O switching in silicon”, Proc. SPIE, vol. 704**,** pp. 32-37, 1986.

[6] OptiBPM by Optiwave Corporation, ver. 7.0, single license, 2005.